Journal of Zhejiang University-SCIENCE B (Biomedicine & Biotechnology)   2023 24(7):650-662
www.jzus.zju.edu.cn; www.springer.com/journal/11585
E-mail: jzus_b@zju.edu.cn

Research Article

https://doi.org/10.1631/jzus.B2200491

Modulating effects of *Astragalus* polysaccharide on immune disorders via gut microbiota and the TLR4/NF-κB pathway in rats with syndrome of dampness stagnancy due to spleen deficiency

Wenxiao ZHAO[1]✉, Chenchen DUAN[1], Yanli LIU[1], Guangying LU[2], Qin LYU[2], Xiumei LIU[3], Jun ZHENG[1], Xuelian ZHAO[1], Shijun WANG[2], Haijun ZHAO[2]✉

[1] *School of Nursing, Shandong University of Traditional Chinese Medicine, Jinan 250355, China*
[2] *College of Traditional Chinese Medicine, Shandong Co-Innovation Center of Classic Traditional Chinese Medicine Formula, Shandong University of Traditional Chinese Medicine, Jinan 250355, China*
[3] *School of Pharmaceutical Sciences, Cheeloo College of Medicine, Shandong University, Jinan 250012, China*

Abstract: The syndrome of dampness stagnancy due to spleen deficiency (DSSD) is relatively common globally. Although the pathogenesis of DSSD remains unclear, evidence has suggested that the gut microbiota might play a significant role. *Radix Astragali*, used as both medicine and food, exerts the effects of tonifying spleen and qi. *Astragalus* polysaccharide (APS) comprises a macromolecule substance extracted from the dried root of *Radix Astragali*, which has many pharmacological functions. However, whether APS mitigates the immune disorders underlying the DSSD syndrome via regulating gut microbiota and the relevant mechanism remains unknown. Here, we used DSSD rats induced by high-fat and low-protein (HFLP) diet plus exhaustive swimming, and found that APS of moderate molecular weight increased the body weight gain and immune organ indexes, decreased the levels of interleukin-1β (IL-1β), IL-6, and endotoxin, and suppressed the Toll-like receptor 4/nuclear factor-κB (TLR4/NF-κB) pathway. Moreover, a total of 27 critical genera were significantly enriched according to the linear discriminant analysis effect size (LEfSe). APS increased the diversity of the gut microbiota and changed its composition, such as reducing the relative abundance of *Pseudoflavonifractor* and *Paraprevotella*, and increasing that of *Parasutterella*, *Parabacteroides*, *Clostridium XIVb*, *Oscillibacter*, *Butyricicoccus*, and *Dorea*. APS also elevated the contents of short-chain fatty acids (SCFAs). Furthermore, the correlation analysis indicated that 12 critical bacteria were related to the body weight gain and immune organ indexes. In general, our study demonstrated that APS ameliorated the immune disorders in DSSD rats via modulating their gut microbiota, especially for some bacteria involving immune and inflammatory response and SCFA production, as well as the TLR4/NF-κB pathway. This study provides an insight into the function of APS as a unique potential prebiotic through exerting systemic activities in treating DSSD.

Key words: *Astragalus* polysaccharide; Gut microbiota; Toll-like receptor 4/nuclear factor-κB (TLR4/NF-κB) pathway; Dampness stagnancy due to spleen deficiency; Immune disorder; Short-chain fatty acid

1 Introduction

According to the theory of traditional Chinese medicine (TCM), the spleen, regarded as the "official of granaries," dominates the transportation and transformation of refined substances in the diet and is the foundation and source of blood biochemistry (Yang and Jia, 2013). Improper diet and prolonged exhaustion will lead to the syndrome of dampness stagnancy due to spleen deficiency (DSSD), which is characterized by a series of symptoms, such as dizziness, fatigue, indigestion, weight loss, loss of appetite, thick and slimy tongue, and edema (Zhao et al., 2017; Liu et al., 2022). DSSD is a common syndrome globally, which often exists alone or accompanying other diseases, with a certain value for disease prognosis (Liu et al., 2022). At present, the pathogenesis of DSSD syndrome remains unclear, while Chinese materia medica with the function of fortifying the spleen and eliminating dampness provide crucial drugs for treatment and prevention.

✉ Wenxiao ZHAO, zhaowx@sdutcm.edu.cn
Haijun ZHAO, haijunzhao@sdutcm.edu.cn

Wenxiao ZHAO, https://orcid.org/0000-0001-7165-5870
Haijun ZHAO, https://orcid.org/0000-0003-0858-7486

Received Oct. 6, 2022; Revision accepted Mar. 28, 2023;
Crosschecked June 12, 2023

Radix Astragali (Huangqi), the dried root of *Astragalus membranaceus* (Fisch.) Bge. or *A. membranaceus* (Fisch.) Bge. var. *Mongholicus* (Bge.) Hsiao, is traditionally considered as Chinese materia medica for its spleen-fortifying and qi-tonifying effects against fatigue, loss of appetite, anemia, infection, and edema, and has been approved as a food resource. *Astragalus* polysaccharide (APS) is a substance containing macromolecules extracted from the dried root of *Radix Astragali*, which are responsible for its therapeutic efficacy (Fu et al., 2014). Modern scientific research has demonstrated that APS possess various pharmacological activities, including immunopotentiation, anti-inflammatory, antioxidant, and antitumor (Zhou et al., 2017; Du et al., 2022). APS is not only widely used in the clinic but also extensively applied as an immunopotentiator in farmed animal industries. Recently, APS has become new raw materials of a dietary supplement for reinforcing body immunity (Song BC et al., 2022).

In our previous studies, we established that APS is the main component of *Radix Astragali* for its spleen-fortifying effect (Zhao et al., 2017); moreover, APS enhances the immune function of rats with DSSD syndrome induced by the method of high-fat and low-protein (HFLP) diet plus exhaustive swimming (Zhao et al., 2019). Numerous studies have suggested that the gut microbiota and their metabolites play an important role in immune disorders and low-grade inflammation triggered by high-fat diet (HFD) intake or exhaustion (Dahl et al., 2020; Dupuit et al., 2021). Research has also confirmed that APS could alleviate HFD-induced metabolic disorders via the gut microbiota and exert an immunomodulatory effect via the Toll-like receptor 4 (TLR4) signaling pathway (Zhou et al., 2017; Hong et al., 2020). However, whether APS mitigates DSSD via regulating the gut microbiota to remedy the immune disorder and the relevant mechanism have not been elucidated.

To further clarify whether the gut microbiota and TLR4 pathway are the therapeutic targets of APS, thus mitigating immune disorders in DSSD syndrome, we investigated the effects of APS on gut microbiota community and their metabolites and the TLR4/nuclear factor-κB (NF-κB) pathway, and identified the changes in critical bacterial genera closely associated with APS treatment.

2 Materials and methods

2.1 Animals

A total of 45 specific pathogen-free Wistar male rats (four weeks old, (120±10) g) were purchased from Beijing Vital River Laboratory Animal Technology Co., Ltd. (Beijing, China). Three animals were housed in each individually ventilated cage at 24 °C and 55% relative humidity. All rats were maintained under standard lighting conditions with free access to regular feed and water.

2.2 Drugs

The APS formula was purchased from Beijing Solarbio Science & Technology Co., Ltd. (Beijing, China), with more than 90% (mass ratio) polysaccharide content. The relative molecular weight and homogeneity of APS were determined using the size exclusion chromatography-multiangle laser light scattering (SEC-MALLS) method and calculated by Astra 5.3.4 software (Waytt Technology, CA, USA). The homogeneities were evaluated by the polydispersity index.

2.3 Animal model and intervention strategy

After 3 d of acclimatization, the rats were randomly divided into five groups: normal group (NG), model group (MG), APS high-dose (APSH) group, APS medium-dose (APSM) group, and APS low-dose (APSL) group, with nine rats per group. Rats in the normal group were fed with AIN-76A purified rodent diet. The other four groups of rats were used to establish the DSSD rat model, which were fed with HFLP diet and given exhaustive swimming once a day for six weeks based on our published method (Zhao et al., 2017). Then, the rats in the APSL, APSM, and APSH groups were administered 300, 600, and 1200 mg/kg APS, respectively, via oral gavage at 1 mL/100 g once a day for two weeks according to our previous study (Zhao et al., 2019). The rats in the normal and model groups were given an equal volume of normal saline. The changes in the body weight of all rats were observed during the experiment. At the end of the eighth week, the rats were fasted for 12 h and anesthetized with isoflurane inhalation. The blood, colon tissue, feces, and cecal contents were collected for future analyses.

2.4 Body weight gain and immune organ index analysis

Body weight gain was defined as the difference between the body weight of rats at the end of the sixth week and the eighth week. The spleen and thymus were cut off and weighed after anesthesia. The spleen/thymus index was calculated as:

$$\text{Spleen/thymus index}=\text{spleen or thymus weight (g)/body weight (g)}\times 100\%. \quad (1)$$

2.5 Measurement of serum IL-1β, IL-6, and plasma endotoxin levels

Serum interleukin-1β (IL-1β) and IL-6 were measured according to the manufacturer's instructions for the enzyme-linked immunosorbent assay (ELISA) kits (Bioss, Beijing, China). The plasma endotoxin was measured according to the instructions of the limulus amoebocyte lysate (LAL) Chromogenic Endotoxin Quantitation kit (Bioendo, Xiamen, China).

2.6 Western blot

Proteins were extracted using radio-immunoprecipitation assay (RIPA) buffer with protease inhibitors from colon tissue, separated on sodium dodecyl sulfate-polyacrylamide gel electrophoresis (SDS-PAGE) gel, and then transferred onto polyvinylidene fluoride (PVDF) membranes (Millipore, Bedford, USA). The membranes were incubated with the primary antibodies overnight and the secondary antibodies for 1 h, followed by the detection of chemiluminescence. Antibody against TLR4 was purchased from Abcam (MA, USA), and antibodies against NF-κB p65, inhibitor of NF-κB-α (IκBα), phospho-IκBα (p-IκBα), and glyceraldehyde-3-phosphate dehydrogenase (GAPDH) were purchased from Cell Signaling Technology (MA, USA). The intensity of the bands was quantified by ImageJ software (https://imagej.net/downloads).

2.7 Gut microbiota detection and analysis

Total genomic DNA was extracted from the feces using a QIAamp DNA Stool Mini kit (Qiagen, Hilden, Germany) according to the manufacturer's directions. The microbial 16S ribosomal DNA (rDNA) V3–V4 region was amplified with indexes and adaptors linked to the universal primers 341F and 806R. The high-throughput sequencing protocol was performed on the Illumina MiSeq PE250 platform at the Realbio Genomics Institute (Shanghai, China).

The chimeric sequences were filtered, and sequences with more than 97% similarity were regarded as the same operational taxonomic units (OTUs) by USEARCH software (https://www.drive5.com/usearch). Alpha and beta diversity analyses were carried out by the Quantitative Insights into Microbial Ecology (QIIME) software (http://qiime.org). The rank sum test for inter-group significant difference analysis was performed to identify species with differences. The linear discriminant analysis (LDA) effect size (LEfSe) analysis was performed to assess the differential species abundance among groups. The Spearman's correlation coefficients were analyzed by R software (https://www.r-project.org).

2.8 Analysis of short-chain fatty acids (SCFAs)

About 50 mg cecal contents were added with 50 μL 15% (volume ratio) phosphoric acid, 125 μg/mL of isohexanoic acid solution, and 400 μL ether, homogenized for 1 min, and grinded for 60 s in a high-throughput tissue grinder. The sample was centrifuged followed by the collection of supernatant liquid for identifying and quantifying short-chain fatty acids (SCFAs) with the gas chromatography-mass spectrometry (GC-MS) system. The metabolite-specific parameters (retention time) of the chromatogram were determined using high-purity chemical standards. The linear regression equation ($R>0.99$) was employed to estimate the concentration of each SCFA from the standard curves obtained using seven different concentrations.

2.9 Statistical analysis

The quantitative data were presented as the mean± standard error of the mean (SEM). All statistical analyses were performed using SPSS 20.0 software (Chicago, USA). If the data met the assumption of homoscedasticity, the significance of differences in the mean value for groups was determined by one-way analysis of variance (ANOVA), followed by the least significant difference (LSD) method for multigroup comparisons. P value of <0.05 was considered statistically significant.

3 Results

3.1 Molecular weight of APS

Three peaks were detected in the differential refractive index (dRI) chromatogram (Fig. S1a), and the molecular weight distribution was shown in Fig. S1b. The molar mass moments and the polydispersity corresponding to each peak were shown in Table S1. The proportion of samples with molecular weight in the range of 0–500×10^3 g/mol was 96.2%, and the number-average molecular weight and the weight-average molecular weight of these samples were 35.8×10^3 and 48.9×10^3 g/mol, respectively.

3.2 Effects of APS on the body weight gain and immune organ indexes

As shown in Figs. 1a and 1b, the body weight gain and the spleen index in the model group were lower than those in the normal group ($P<0.01$), and the thymus index showed a downward trend compared with the normal group (Fig. 1c). Compared with the model group, the body weight gain, spleen index, and thymus index in the APS groups with different doses were significantly increased.

3.3 Effects of APS on IL-1β, IL-6, and endotoxin contents, and protein expression levels in the TLR4/NF-κB pathway

The contents of IL-1β, IL-6, and endotoxin in the model group were higher than those in the normal group ($P<0.01$; Figs. 2a–2c). The IL-1β and IL-6 contents were significantly decreased in each APS group compared with the model group ($P<0.01$; Figs. 2a and 2b). The endotoxin content in each APS group showed a reduction compared to the model group, although the difference was not significant (Fig. 2c). As shown in Figs. 2d and 2e, the expression levels of TLR4, NF-κB p65, p-IκBα, and p-IκBα/IκBα in the model group were increased when compared with the normal group ($P<0.01$), and the expression level of IκBα was decreased when compared to the normal group ($P<0.01$), while APS in different doses significantly reduced the expression levels of NF-κB p65, p-IκBα and p-IκBα/IκBα compared with the model group ($P<0.01$). Compared with the model group, APSM and APSH decreased the expression level of TLR4 ($P<0.01$), while APSM increased the expression level of IκBα ($P<0.01$).

3.4 Effect of APS administration on the gut microbiota

3.4.1 Changes of the taxonomic abundance and diversity of gut microbiota by APS

The species taxonomic composition of gut microbiota at the phylum level was observed, and nine major phyla were shown in Fig. 3a. Firmicutes and Bacteroidetes were the most abundant phyla. An increase in relative abundance of Firmicutes and Proteobacteria, and a reduction in Bacteroidetes and Verrucomicrobia in the model group were detected compared with the normal group. APS remarkably enriched the relative abundance of Proteobacteria; moreover, APS slightly increased the relative abundance of Bacteroidetes and decreased that of Firmicutes compared with the model group.

For alpha diversity, the Shannon and Simpson indexes were analyzed (Figs. 3b and 3c). Compared with the model group, the Shannon index of the APSM group was increased ($P<0.05$). Compared with the normal group, the Shannon and Simpson indexes of APSH group ($P<0.05$) and APSM group ($P<0.01$) were both significantly increased. For beta diversity, the analysis of similarities (Anosim) using unweighted UniFrac and the non-metric multidimensional scaling (NMDS) analysis were calculated to assess the difference in community composition between different

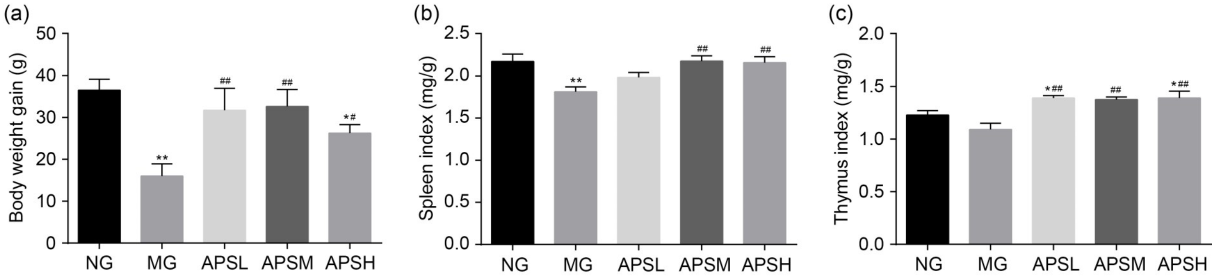

Fig. 1 Effects of APS on the body weight gain and immune organ indexes. (a) Body weight gain. (b) Spleen index. (c) Thymus index. All data were expressed as mean±SEM, *n*=9. * $P<0.05$, ** $P<0.01$ vs. NG; $^{\#}$ $P<0.05$, $^{\#\#}$ $P<0.01$ vs. MG. APS: *Astragalus* polysaccharide; APSH: APS high-dose group; APSL: APS low-dose group; APSM: APS medium-dose group; MG: model group; NG: normal group; SEM: standard error of the mean.

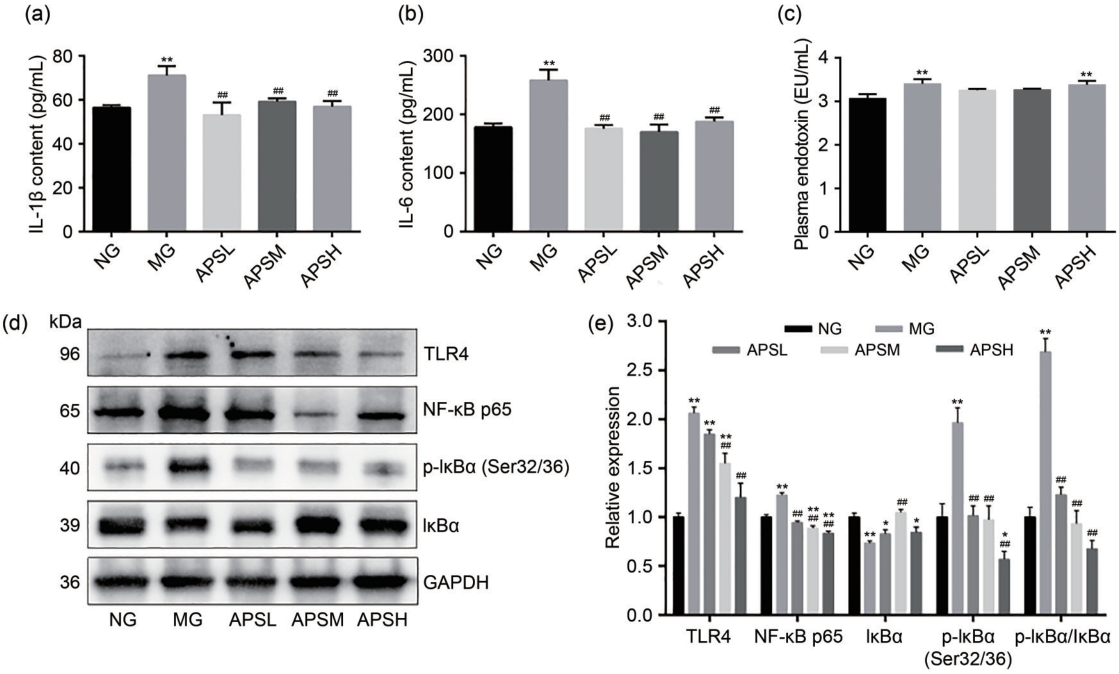

Fig. 2 Effects of APS on the contents of IL-1β, IL-6, endotoxin, and the protein expression of TLR4/NF-κB pathway. (a) IL-1β content, and *n*=6. (b) IL-6 content, and *n*=8. (c) Plasma endotoxin content, and *n*=5. (d, e) Protein levels were detected by western blot in the colon tissue, and the relative expression levels were quantified; *n*=3. All data were expressed as mean±SEM. * *P*<0.05, ** *P*<0.01 vs. NG; $^{\#}$ *P*<0.05, $^{\#\#}$ *P*<0.01 vs. MG. APS: *Astragalus* polysaccharide; APSH: APS high-dose group; APSL: APS low-dose group; APSM: APS medium-dose group; EU: endotoxin unit; GAPDH: glyceraldehyde-3-phosphate dehydrogenase; NF-κB: nuclear factor-κB; IκBα: inhibitor of NF-κB-α; IL-1β: interleukin-1β; MG: model group; NG: normal group; p-IκBα: phosphor-IκBα; SEM: standard error of the mean; Ser: serine; TLR4: Toll-like receptor 4.

samples. The Anosim result showed that the difference in inter-group was greater than that in the intra-group (*R*=0.442, *P*=0.001; Fig. 3d). The NMDS result indicated the degree of difference among each sample (Fig. 3e).

3.4.2 Effect of APS on critical phylotype of the gut microbiota in different groups

3.4.2.1 Inter-group difference and LEfSe analysis of gut microbiota

We found 290 OTUs with significant differences among different groups by the rank-sum test, and the principal component analysis (PCA) score plot based on the differential OTUs was shown in Fig. 4a.

The differentially abundant species in the cladogram created by LEfSe analysis were shown in Fig. 4b, while Fig. 4c illustrated the LDA scores of differential species and a total of 27 significantly different species at the genus level were identified. The genus *Pseudoflavonifractor* was enriched in the model group. Meanwhile, there was higher abundance of genera *Oscillibacter*, *Lactonifactor*, *Butyricicoccus*, and *Staphylococcus* in the APSH group, *Parabacteroides*, *Clostridium XI*, *Roseburia*, *Clostridium XIVb*, *Flavonifractor*, *Pseudomonas*, *Gemella*, *Bilophila*, and *Dorea* in the APSM group, and *Helicobacter*, *Ruminococcus*, *Anaeroplasma*, and *Alistipes* in the APSL group (lg(LDA score)>3). *Paraprevotella*, *Ruminococcus 2*, *Psychrobacter*, *Lactobacillus*, *Eubacterium*, *Barnesiella*, and *Parasutterella* were enriched in the normal group (lg(LDA score)>3).

3.4.2.2 Comparison of relative abundance of the critical bacterial genera among groups

We performed a pairwise comparison analysis of variance on the enriched intestinal flora in the model and APS administration groups. The relative abundance of the critical bacterial genera among different groups was shown in Fig. 5. In the model group, the relative abundance of genera *Pseudoflavonifractor*, *Flavonifractor*, and *Alistipes* was increased (*P*<0.05), and that of *Eubacterium*, *Barnesiella*, *Lactobacillus*, *Psychrobacter*, *Parasutterella*, and *Corynebacterium* was decreased compared with the normal group (*P*<0.05). APS administration groups, especially APSH group and APSM group, decreased the relative abundance of *Pseudoflavonifractor* and increased that of *Parasutterella*

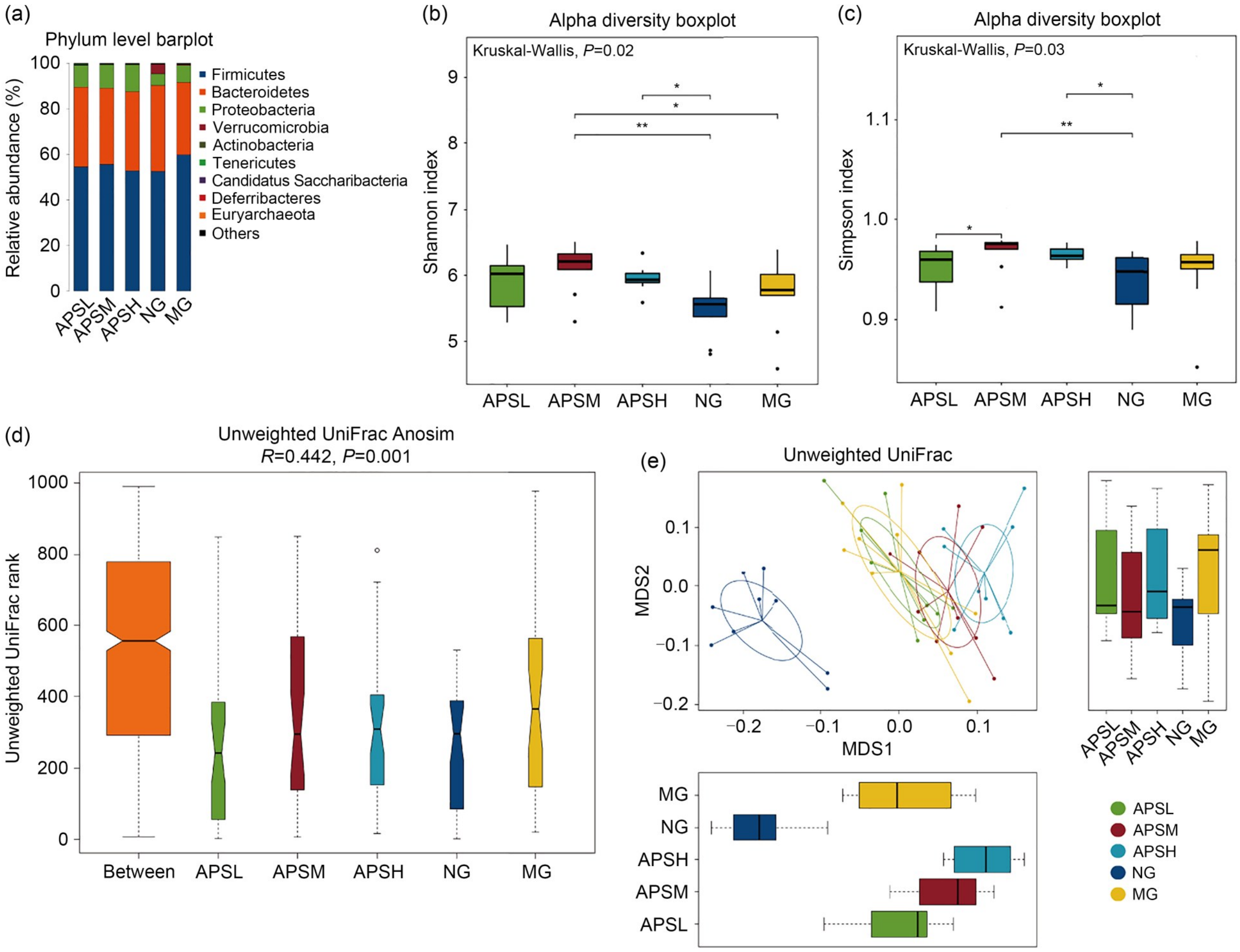

Fig. 3 Effects of APS on the taxonomic classification abundance and diversity of the gut microbiota of rats. (a) Relative abundance of the dominant bacteria in the rat feces at the phylum level. (b) Shannon diversity index. (c) Simpson diversity index. (d) Unweighted UniFrac Anosim analysis between the groups, where *R*>0 indicates significant inter-group differences compared with the intra-group. (e) NMDS analysis by unweighted UniFrac distance, where a greater distance between two samples implies a higher difference in species composition. All data were expressed as mean±SEM, *n*=9. * *P*<0.05, ** *P*<0.01. Anosim: analysis of similarities; APS: *Astragalus* polysaccharide; APSH: APS high-dose group; APSL: APS low-dose group; APSM: APS medium-dose group; MDS: multidimensional scaling; MG: model group; NG: normal group; NMDS: non-metric multidimensional scaling; SEM: standard error of the mean.

and *Gemella* compared with the model group (*P*<0.05). The relative abundance of *Anaeroplasma* in the APSL group, relative abundance of *Parabacteroides*, *Clostridium XIVb*, *Roseburia*, *Pseudomonas*, and *Dorea* in the APSM group, and relative abundance of *Oscillibacter*, *Butyricicoccus*, and *Staphylococcus* in the APSH group increased compared with the model group (*P*<0.05). Additionally, the abundance of *Barnesiella*, *Lactobacillus*, and *Corynebacterium* showed different degrees of contrary variation tendency in the model rats after APS administration, although no significant difference was indicated. The relative abundance of *Paraprevotella* in the APSH and APSM groups was decreased compared to the normal group (*P*<0.05).

3.4.3 Correlation analyses among significant differential genera, body weight gain, and immune organ indexes

The correlation analysis found that 12 of 27 significant differential genera were associated with the body weight gain and the immune organ indexes. As shown in Fig. 6, *Pseudoflavonifractor* was negatively correlated with the body weight gain (*P*<0.01) and the spleen index (*P*<0.05). At the same time, *Paraprevotella* showed a negative correlation with the spleen index

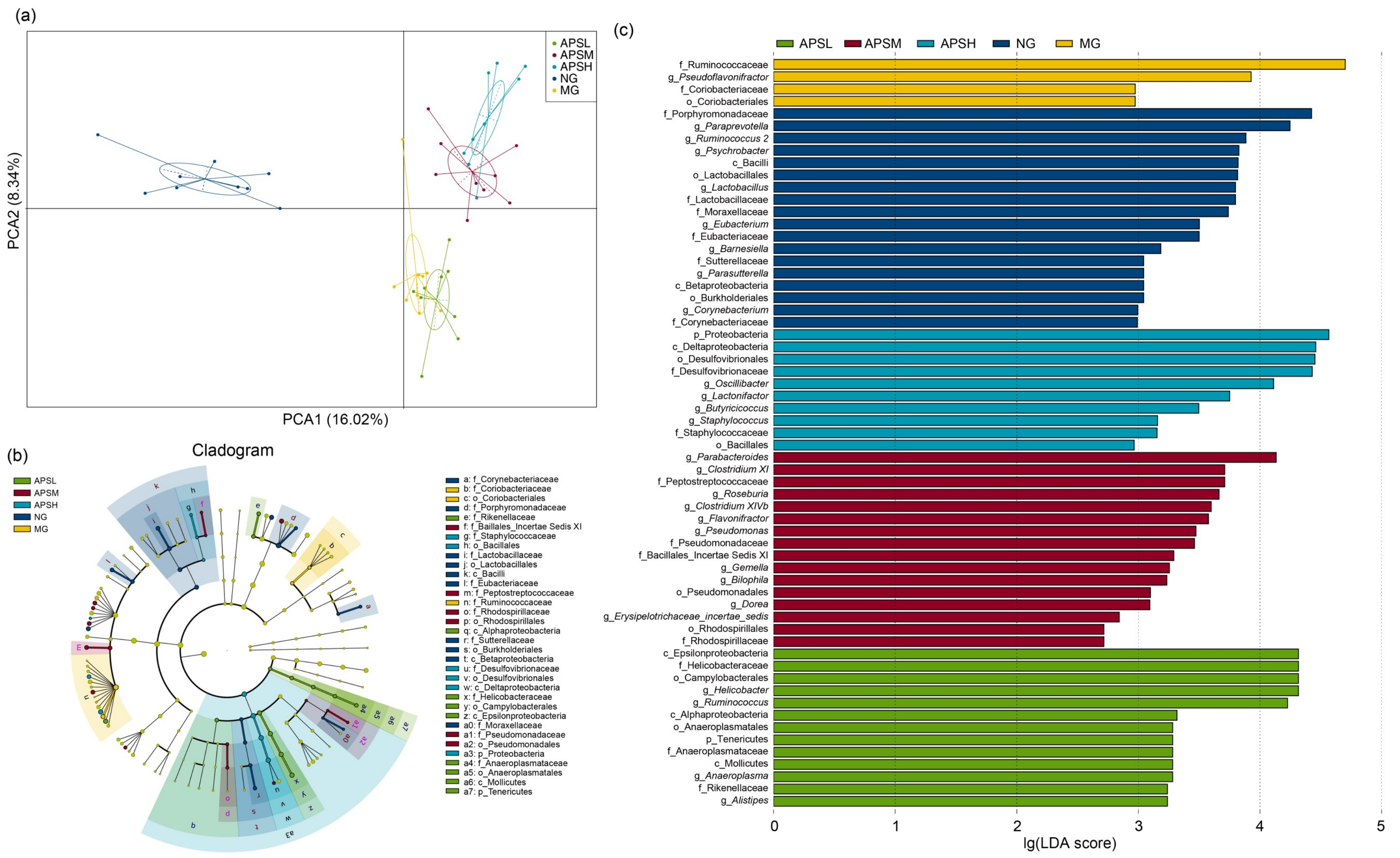

Fig. 4 Inter-group difference and LEfSe analyses of gut microbiota. (a) PCA score plot based on the differential OTUs, with the contribution of principal component to the sample difference represented on the axis. (b) Taxonomic cladogram based on the LEfSe analysis. (c) Histogram of LDA scores according to the LEfSe analysis, with the LDA score representing the impact of the significantly differential species. APSH: *Astragalus* polysaccharide (APS) high-dose group; APSL: APS low-dose group; APSM: APS medium-dose group; LEfSe: linear discriminant analysis (LDA) effect size; MG: model group; NG: normal group; OTUs: operational taxonomic units; PCA: principal component analysis.

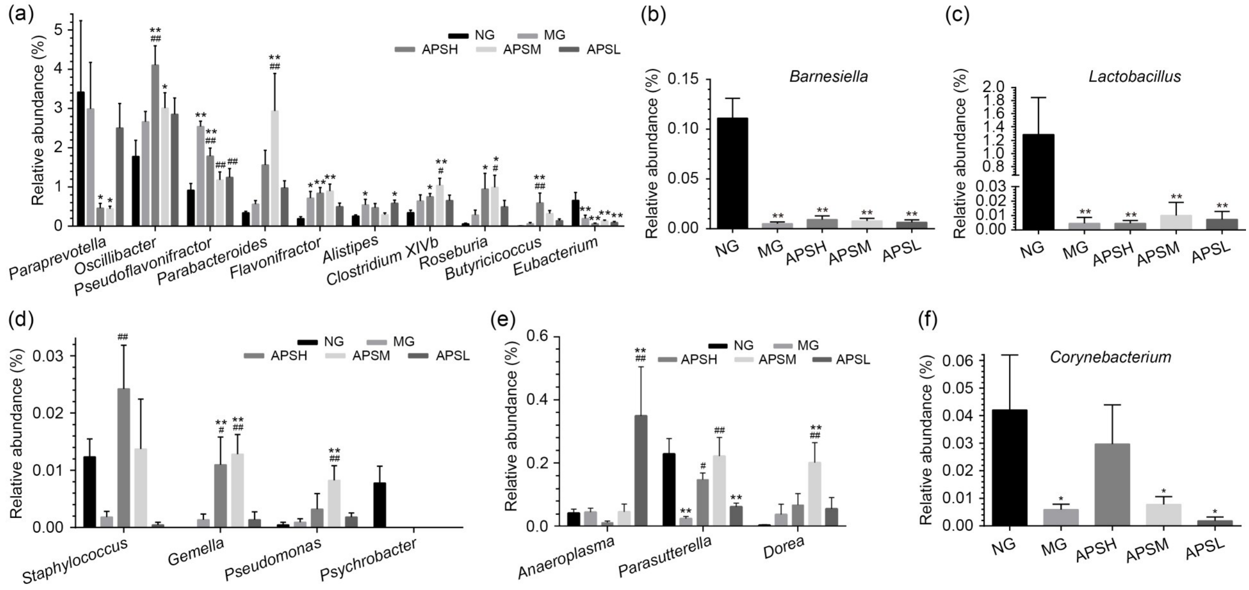

Fig. 5 Relative abundance of key bacterial genera. The differences in the abundance of these bacteria were evidenced to be significant among groups by LEfSe analysis (P<0.05). (a) Relative abundance of *Paraprevotella*, *Oscillibacter*, *Pseudoflavonifractor*, *Parabacteroides*, *Flavonifractor*, *Alistipes*, *Clostridium XIVb*, *Roseburia*, *Butyricicoccus*, and *Eubacterium*. (b) Relative abundance of *Barnesiella*. (c) Relative abundance of *Lactobacillus*. (d) Relative abundance of *Staphylococcus*, *Gemella*, *Pseudomonas*, and *Psychrobacter*. (e) Relative abundance of *Anaeroplasma*, *Parasutterella*, and *Dorea*. (f) Relative abundance of *Corynebacterium*. All data were expressed as mean±SEM, n=9. * P<0.05, ** P<0.01 vs. NG; $^{\#}$ P<0.05, $^{\#\#}$ P<0.01 vs. MG. APSH: *Astragalus* polysaccharide (APS) high-dose group; APSL: APS low-dose group; APSM: APS medium-dose group; LEfSe: linear discriminant analysis effect size; MG: model group; NG: normal group; SEM: standard error of the mean.

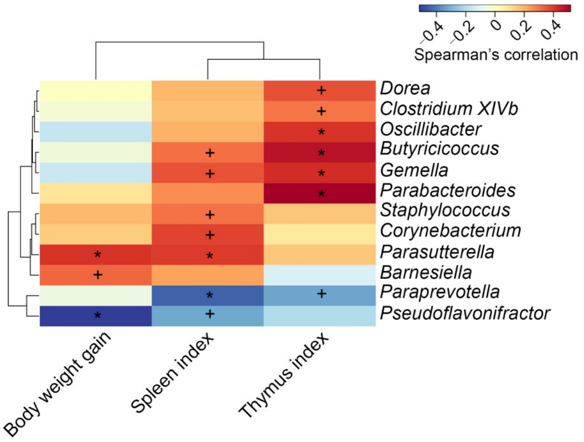

Fig. 6 Heatmap of Spearman's correlation analysis among differential genera, body weight gain, and immune organ indexes. The correlation coefficient was represented by colors ranging from blue (negative correlation) to red (positive correlative). Significant correlation was indicated as $^{+}$ P<0.05 and * P<0.01.

(P<0.01) and thymus index (P<0.05). In contrast, *Parasutterella* (P<0.01) and *Barnesiella* (P<0.05) were positively correlated with the body weight gain. Nine genera were positively associated with the spleen index and/or thymus index, including *Dorea*, *Clostridium XIVb*, *Oscillibacter*, *Butyricicoccus*, *Gemella*, *Parabacteroides*, *Staphylococcus*, *Corynebacterium*, and *Parasutterella* (P<0.05).

3.5 Effect of APS on SCFA production

As shown in Table 1, the contents of seven SCFAs decreased to varying degrees, and the differences in the contents of propionic acid (P<0.05), butyric acid, valeric acid, isobutyric acid, and isovaleric acid (P<0.01) in the model group were statistically significant compared with the normal group. Compared with the model group, APS increased the levels of six SCFAs to some extent, except acetic acid. The content of caproic acid in each APS group (P<0.01), isobutyric acid in the APSL group (P<0.01), and isovaleric acid in the APSL and APSH groups (P<0.05) were higher than those in the model group.

4 Discussion

Earlier studies found that the pharmacological effects of TCM polysaccharides are closely related to their molecular weight (Biao et al., 2020; Li Y et al.,

Table 1 Effects of APS on production of short-chain fatty acids

Group	Acetic acid (μg/g)	Propionic acid (μg/g)	Butyric acid (μg/g)	Valeric acid (μg/g)	Caproic acid (μg/g)	Isobutyric acid (μg/g)	Isovaleric acid (μg/g)
NG	905.06±111.15	445.81±87.42	309.65±65.83	63.93±15.81	1.11±0.09	59.80±7.04	37.85±6.77
MG	756.63±74.89	254.98±6.52*	123.43±12.56**	28.99±2.11**	0.95±0.09	34.57±4.62**	20.85±1.72**
APSL	627.56±79.62*	320.72±50.52	170.35±23.84*	39.98±6.57	1.57±0.11$^{*\#\#}$	56.37±4.32$^{\#\#}$	33.99±3.29$^{\#}$
APSM	730.51±40.54	339.48±65.79	177.82±35.73*	39.08±7.77*	1.62±0.17$^{**\#\#}$	44.63±5.11*	29.84±5.00
APSH	722.14±68.48	381.28±39.73	203.59±41.14	48.14±5.95	1.70±0.14$^{**\#\#}$	47.97±3.95	33.39±2.57$^{\#}$

All data were expressed as mean±SEM, n=6. * P<0.05, ** P<0.01 vs. NG; $^{\#}$ P<0.05, $^{\#\#}$ P<0.01 vs. MG. APS: *Astragalus* polysaccharide; APSH: APS high-dose group; APSL: APS low-dose group; APSM: APS medium-dose group; NG: normal group; MG: model group; SEM: standard error of the mean.

2020). Most reported APS had a molecular weight of 8.7–4800.0 kDa, with the largest percentage of 20–40 kDa polysaccharides in the Inner Mongolia APS (Jin et al., 2014; Sheng et al., 2021). Among them, APS with moderate molecular weight provided the most potent effects of immunomodulation (Jiang et al., 2016; Li K et al., 2020). The average molecular weight of APS used in this study was 35.8×10^{3} g/mol, which is similar to the reported result. We found that APS increased the body weight gain and the immune organ indexes of model rats, and reduced the levels of endotoxin, IL-1β, and IL-6, which suggested that APS alleviated the immune disorders of rats with DSSD syndrome and were consistent with the findings of our previous study (Zhao et al., 2019).

The gut microbiota acts as a central signaling hub that integrates environmental factors (e.g., diet, exercise) with immune signals, and the microorganisms or their metabolites stimulate the TLRs on the gut epithelium and trigger downstream NF-κB to regulate the immune response (Thaiss et al., 2016; Lu et al., 2022; Zhao et al., 2022). Moreover, studies found that *A. membranaceus* polysaccharides can modulate the gut microbiota to alleviate diabetic symptoms in db/db mice and non-alcoholic fatty liver disease in rats (Song QB et al., 2022; Zhong et al., 2022). Given the vital roles of gut microbiota and the reported prebiotic effects of APS, we evaluated the regulatory effects of APS on the gut microbiota and TLR4/NF-κB pathway in rats with DSSD syndrome. We found that APS increased the richness and diversity and notably changed the classification of the gut microbiota of rats with DSSD syndrome, which agrees with the finding of modulation effect of APS on gut microbiota. Moreover, we found that APS decreased the expression levels of TLR4, NF-κB p65, and p-IκBα, and increased the IκBα expression level, which suggests that APS inhibited the activation of TLR4/NF-κB signaling pathway and reduced the production of inflammatory factors.

Firmicutes and Bacteroidetes are two main phyla in the gut microbiota of both rats and humans. Most studies found that a reduction in Bacteroidetes and an increase in Firmicutes were associated with obesity, type 2 diabetes mellitus (T2DM), and other metabolic diseases (Turnbaugh et al., 2006; Crovesy et al., 2020; Zhu et al., 2020), which is consistent with our result. We found that APS slightly increased the reduction in Bacteroidetes and decreased the increase in Firmicutes of the DSSD rats, which did induce some critical changes in bacterial abundance. Furthermore, the relative abundance of Proteobacteria was increased in the model group and APS administration groups. The predominance of Proteobacteria in the gut of patients with IBD, obesity, and T2DM has been known (Massier et al., 2020; Oddi et al., 2020; Putignani et al., 2021); however, there are complex interactions among different genera of gut microbiota, and the role of different bacteria from the same phylum or genus might be different; the diversity of disease course and presentation may represent different levels of microbial involvement in different individuals. An increase in the relative abundance of Proteobacteria in the APS administration groups may be due to a decrease in the relative abundance of other unprofitable strains.

We found that APS reversed the increase in the relative abundance of *Pseudofalvonifractor* and the decrease in the relative abundance of *Parasutterella*. Moreover, *Pseudofalvonifractor* was negatively correlated with the body weight gain and the spleen index, whereas *Parasutterella* was positively correlated with the body weight gain and the spleen index. *Pseudofalvonifractor* belongs to the family Ruminococcaceae and phylum Firmicutes. Studies found that a higher abundance of *Pseudoflavonifractor* contributes to losing weight (Louis et al., 2016), and the downregulation of *Pseudoflavonifractor* was associated with increase in the proportion of T cells in tumor-infiltrating lymphocytes (Messaoudene et al., 2022). These findings are consistent with our results. Research showed that *Parasutterella* from the phylum Proteobacteria is the member of the core gut microbiota and contributes to lipid metabolic functionalities (Ju et al., 2019); moreover, *Parasutterella* was associated with the intestinal inflammatory response (Wu et al., 2022). Polysaccharide-rich extracts could reverse the microbiota dysbiosis to improve inflammatory factor levels by increasing the abundance of *Parasutterella* (Li MX et al., 2020). Our results agreed with the above findings. Therefore, changes in the abundance of *Pseudoflavonifractor* and *Parasutterella* might be among the reasons for abnormal immune response and weight loss, and are also regarded as two kinds of bacterial indexes in estimating the pathological status of rats with DSSD syndrome and two of the target bacteria during APS treatment.

We also found that APS intervention slightly reversed the reduction in the abundance of *Barnesiella*, *Lactobacillus*, and *Corynebacterium* genera in model rats, which were enriched in normal rats. Furthermore, the correlation analysis suggested that *Barnesiella* of Bacteroidetes was positively correlated with body weight gain. *Barnesiella* exerts the effect of competitive inhibition of pathogens, immune regulation, and anti-inflammatory protection (Ubeda et al., 2013; Weiss et al., 2014), which helps to produce butyric acid, isobutyric acid, and a smaller amount of propionic, acetic, and succinic acids (Sakamoto et al., 2009). The genus *Lactobacillus* is a diverse group and includes many species considered as probiotics (Goldstein et al., 2015). The reported effects of these bacteria are consistent with our results. Besides *Parasutterella*, eight genera including *Corynebacterium*, *Staphylococcus*, *Dorea*, *Butyricicoccus*, *Oscillibacter*, *Gemella*, *Parabacteroides*, and *Clostridium XIVb* were enriched in the APS intervention groups in this study, which are gut microbiome associated with immune or inflammatory processes (Bernard, 2012; Paharik and Horswill, 2016; Zaidi et al., 2018). The genus *Butyricicoccus* of the family Ruminococcaceae and phylum Firmicutes is a butyrogenic bacterium, and butyrate is involved in the regulation of inflammatory cytokines (Shang et al., 2016; Zhang et al., 2017). In addition, the levels of *Butyricicoccus* and *Oscillibacter* were related to intestinal inflammatory response (Devriese et al., 2017; Wu MN et al., 2019). *Parabacteroides* species include a variety of probiotics, such as *Parabacteroides goldsteinii* and *Parabacteroides distasonis*, which were negatively correlated with obesity, metabolic dysfunctions, and inflammation (Wang et al., 2019; Wu TR et al., 2019). *Parabacteroides* and *Clostridium XIVb* are also SCFA-producing bacteria (Wang et al., 2019; Lei et al., 2021). These bacteria or their metabolites might play positive roles in activating immune function and metabolism in the therapeutic process of APS.

In this study, the abundance of enriched *Paraprevotella* in normal rats was decreased in the APSM and APSH groups, which was negatively correlated with the immune organ index. Hibberd et al. (2019) reported that *Paraprevotella* was highly abundant in overweight and obese human adults and also positively correlated to body fat mass, which suggests that its increased abundance may be detrimental to health. Yuan et al. (2021) showed that dysbiosis of gut microbiota was presented in the metabolically healthy obese children, and the abundance of *Paraprevotella* was positively correlated with serum IL-6. Therefore, a high abundance of *Paraprevotella* may be a remedial response to poor health, and APS could reverse this change.

SCFAs as metabolites of intestinal microbiota play a beneficial role in modulating host immune response, providing energy for colonic epithelium, mitigating chronic inflammation and metabolism as signaling molecules, and suppressing the production of pro-inflammatory cytokines (Koh et al., 2016; Parada Venegas et al., 2019). Ming et al. (2022) found that APS treatment inhibited LPS-induced inflammation in mice, which was partly caused by increased abundance of SCFA-producing genera and the serum concentrations of butyrate and propionate. Song QB et al. (2022) reported that *A. membranaceus* polysaccharides increased the production of fecal SCFAs in db/db mice. In our study, APS increased the contents of butyric acid, valeric acid, caproic acid, isobutyric acid, and isovaleric acid in the model group, which was consistent with these earlier reports. The promoting effects of APS on SCFA production were supported by the observation of enriched *Barnesiella*, *Roseburia*, *Ruminococcus*, *Parabacteroides*, *Butyricicoccus*, and *Clostridium XIVb*. The genus *Roseburia* has butyrate-producing capacity and is an anti-inflammatory factor that can decrease the risk of metabolic and inflammatory diseases (Louis and Flint, 2009; Tamanai-Shacoori et al., 2017). *Ruminococcus*, *Clostridium XIVb*, and *Roseburia* all belong to the family Lachnospiraceae, and many bacteria from this family are known as potent SCFA producers (Wei et al., 2018; Kim et al., 2020). Therefore, our data illustrated that these SCFAs-producing bacteria might play a significantly positive role in the process of APS to relieve the DSSD syndrome.

5 Conclusions

Overall, the results of this study indicated that APS could ameliorate the immune disorders in rats with DSSD syndrome induced by HFLP diet plus exhaustive swimming via modulating the gut microbiota and their metabolites, as well as the TLR4/NF-κB pathway. We supposed that the effect of APS on DSSD rats was closely related to some bacteria, which were associated with the production of SCFAs and immune and inflammatory responses. Therefore, we suggest that modifying the gut microbiota might be one of the mechanisms to attenuate the DSSD syndrome. This study provides a new insight into the roles of APS as a unique potential prebiotic, exerting systemic activities from gut microbiota perspective, which might be helpful in the development of health products to provide more effective therapies for the DSSD syndrome.

Acknowledgments

This work was supported by the National Natural Science Foundation of China (No. 81903947) and the Key Research and Development Project of Shandong Province (No. 2019GSF108209), China.

Author contributions

Wenxiao ZHAO conceptualized and designed the study, wrote the initial draft, and provided financial support. Chenchen DUAN, Guangying LU, Qin LYU, Xiumei LIU, Jun ZHENG, and Xuelian ZHAO performed the experiment and analyzed the data. Yanli LIU, Shijun WANG, and Haijun ZHAO coordinated the research activity execution. All authors have read and approved the final manuscript, and therefore, have full access to all the data in the study and take responsibility for the integrity and security of the data.

Compliance with ethics guidelines

Wenxiao ZHAO, Chenchen DUAN, Yanli LIU, Guangying LU, Qin LYU, Xiumei LIU, Jun ZHENG, Xuelian ZHAO, Shijun WANG, and Haijun ZHAO declare that they have no conflict of interest.

All experimental procedures in this study were approved by the Animal Ethics Committee of Shandong University of Traditional Chinese Medicine (No. SDUTCM20210315009). All institutional and national guidelines for the care and use of laboratory animals were followed.

References

Bernard K, 2012. The genus *Corynebacterium* and other medically relevant coryneform-like bacteria. *J Clin Microbiol*, 50(10):3152-3158.
https://doi.org/10.1128/jcm.00796-12

Yuan B, Han JN, Cheng YL, et al., 2020. Identification and characterization of antioxidant and immune-stimulatory polysaccharides in flaxseed hull. *Food Chem*, 315:126266.
https://doi.org/10.1016/j.foodchem.2020.126266

Crovesy L, Masterson D, Rosado EL, 2020. Profile of the gut microbiota of adults with obesity: a systematic review. *Eur J Clin Nutr*, 74(9):1251-1262.
https://doi.org/10.1038/s41430-020-0607-6

Dahl WJ, Rivero Mendoza D, Lambert JM, 2020. Chapter eight – diet, nutrients and the microbiome. *In*: Sun J (Ed.), Progress in Molecular Biology and Translational Science, Vol. 171. Elsevier, the Netherlands, p.237-263.
https://doi.org/10.1016/bs.pmbts.2020.04.006

Devriese S, Eeckhaut V, Geirnaert A, et al., 2017. Reduced mucosa-associated *Butyricicoccus* activity in patients with ulcerative colitis correlates with aberrant claudin-1 expression. *J Crohns Colitis*, 11(2):229-236.
https://doi.org/10.1093/ecco-jcc/jjw142

Du Y, Wan HT, Huang P, et al., 2022. A critical review of *Astragalus* polysaccharides: from therapeutic mechanisms to pharmaceutics. *Biomed Pharmacother*, 147:112654.
https://doi.org/10.1016/j.biopha.2022.112654

Dupuit M, Chavanelle V, Chassaing B, et al., 2021. The TOTUM-63 supplement and high-intensity interval training combination limits weight gain, improves glycemic control, and influences the composition of gut mucosa-associated bacteria in rats on a high fat diet. *Nutrients*, 13(5):1569.
https://doi.org/10.3390/nu13051569

Fu J, Wang ZH, Huang LF, et al., 2014. Review of the botanical characteristics, phytochemistry, and pharmacology of *Astragalus membranaceus* (Huangqi). *Phytother Res*, 28(9):1275-1283.
https://doi.org/10.1002/ptr.5188

Goldstein EJC, Tyrrell KL, Citron DM, 2015. *Lactobacillus* species: taxonomic complexity and controversial susceptibilities. *Clin Infect Dis*, 60(Suppl 2):S98-S107.
https://doi.org/10.1093/cid/civ072

Hibberd AA, Yde CC, Ziegler ML, et al., 2019. Probiotic or synbiotic alters the gut microbiota and metabolism in a randomised controlled trial of weight management in overweight adults. *Benef Microbes*, 10(2):121-135.
https://doi.org/10.3920/bm2018.0028

Hong Y, Li BB, Zheng NN, et al., 2020. Integrated metagenomic and metabolomic analyses of the effect of *Astragalus* polysaccharides on alleviating high-fat diet-induced

metabolic disorders. *Front Pharmacol*, 11:833.
https://doi.org/10.3389/fphar.2020.00833

Jiang YP, Qi XH, Gao K, et al., 2016. Relationship between molecular weight, monosaccharide composition and immunobiologic activity of *Astragalus* polysaccharides. *Glycoconj J*, 33(5):755-761.
https://doi.org/10.1007/s10719-016-9669-z

Jin ML, Zhao K, Huang QS, et al., 2014. Structural features and biological activities of the polysaccharides from *Astragalus membranaceus*. *Int J Biol Macromol*, 64:257-266.
https://doi.org/10.1016/j.ijbiomac.2013.12.002

Ju TT, Kong JY, Stothard P, et al., 2019. Defining the role of *Parasutterella*, a previously uncharacterized member of the core gut microbiota. *ISME J*, 13(6):1520-1534.
https://doi.org/10.1038/s41396-019-0364-5

Kim J, Choi JH, Ko G, et al., 2020. Anti-inflammatory properties and gut microbiota modulation of *Porphyra tenera* extracts in dextran sodium sulfate-induced colitis in mice. *Antioxidants*, 9(10):988.
https://doi.org/10.3390/antiox9100988

Koh A, de Vadder F, Kovatcheva-Datchary P, et al., 2016. From dietary fiber to host physiology: short-chain fatty acids as key bacterial metabolites. *Cell*, 165(6):1332-1345.
https://doi.org/10.1016/j.cell.2016.05.041

Lei YY, Tang L, Liu S, et al., 2021. Parabacteroides produces acetate to alleviate heparanase-exacerbated acute pancreatitis through reducing neutrophil infiltration. *Microbiome*, 9:115.
https://doi.org/10.1186/s40168-021-01065-2

Li K, Cao YX, Jiao SM, et al., 2020. Structural characterization and immune activity screening of polysaccharides with different molecular weights from Astragali Radix. *Front Pharmacol*, 11:582091.
https://doi.org/10.3389/fphar.2020.582091

Li MX, Guo CL, Wang YQ, et al., 2020. *Nostoc sphaeroids* Kütz polysaccharide and powder enrich a core bacterial community on C57BL/6j mice. *Int J Biol Macromol*, 162:1734-1742.
https://doi.org/10.1016/j.ijbiomac.2020.08.026

Li Y, Qin GYX, Cheng C, et al., 2020. Purification, characterization and anti-tumor activities of polysaccharides from *Ecklonia kurome* obtained by three different extraction methods. *Int J Biol Macromol*, 150:1000-1010.
https://doi.org/10.1016/j.ijbiomac.2019.10.216

Liu J, Qiao B, Tan ZJ, 2022. Progress in modern research on substance of spleen qi deficiency in Chinese medicine. *World Chin J Digestol*, 30(16):693-700 (in Chinese).
https://doi.org/10.11569/wcjd.v30.i16.693

Louis P, Flint HJ, 2009. Diversity, metabolism and microbial ecology of butyrate-producing bacteria from the human large intestine. *FEMS Microbiol Lett*, 294(1):1-8.
https://doi.org/10.1111/j.1574-6968.2009.01514.x

Louis S, Tappu RM, Damms-Machado A, et al., 2016. Characterization of the gut microbial community of obese patients following a weight-loss intervention using whole metagenome shotgun sequencing. *PLoS ONE*, 11(2):e0149564.
https://doi.org/10.1371/journal.pone.0149564

Lu YT, Liu HY, Yang K, et al., 2022. A comprehensive update: gastrointestinal microflora, gastric cancer and gastric premalignant condition, and intervention by traditional Chinese medicine. *J Zhejiang Univ-Sci B (Biomed & Biotechnol)*, 23(1):1-18.
https://doi.org/10.1631/jzus.B2100182

Massier L, Chakaroun R, Tabei S, et al., 2020. Adipose tissue derived bacteria are associated with inflammation in obesity and type 2 diabetes. *Gut*, 69(10):1796-1806.
https://doi.org/10.1136/gutjnl-2019-320118

Messaoudene M, Pidgeon R, Richard C, et al., 2022. A natural polyphenol exerts antitumor activity and circumvents anti-PD-1 resistance through effects on the gut microbiota. *Cancer Discov*, 12(4):1070-1087.
https://doi.org/10.1158/2159-8290.Cd-21-0808

Ming K, Zhuang S, Ma N, et al., 2022. *Astragalus* polysaccharides alleviates lipopolysaccharides-induced inflammatory lung injury by altering intestinal microbiota in mice. *Front Microbiol*, 13:1033875.
https://doi.org/10.3389/fmicb.2022.1033875

Oddi S, Huber P, Rocha Faria Duque AL, et al., 2020. Breast-milk derived potential probiotics as strategy for the management of childhood obesity. *Food Res Int*, 137:109673.
https://doi.org/10.1016/j.foodres.2020.109673

Paharik AE, Horswill AR, 2016. The staphylococcal biofilm: adhesins, regulation, and host response. *Microbiol Spectr*, 4(2):VMBF-0022-2015.
https://doi.org/10.1128/microbiolspec.VMBF-0022-2015

Parada Venegas D, de la Fuente MK, Landskron G, et al., 2019. Short chain fatty acids (SCFAs)-mediated gut epithelial and immune regulation and its relevance for inflammatory bowel diseases. *Front Immunol*, 10:277.
https://doi.org/10.3389/fimmu.2019.00277

Putignani L, Oliva S, Isoldi S, et al., 2021. Fecal and mucosal microbiota profiling in pediatric inflammatory bowel diseases. *Eur J Gastroenterol Hepatol*, 33(11):1376-1386.
https://doi.org/10.1097/meg.0000000000002050

Sakamoto M, Takagaki A, Matsumoto K, et al., 2009. *Butyricimonas synergistica* gen. nov., sp. nov. and *Butyricimonas virosa* sp. nov., butyric acid-producing bacteria in the family '*Porphyromonadaceae*' isolated from rat faeces. *Int J Syst Evol Microbiol*, 59(7):1748-1753.
https://doi.org/10.1099/ijs.0.007674-0

Shang HX, Sun J, Chen YQ, 2016. *Clostridium butyricum* CGMCC0313.1 modulates lipid profile, insulin resistance and colon homeostasis in obese mice. *PLoS ONE*, 11(4):e0154373.
https://doi.org/10.1371/journal.pone.0154373

Sheng ZL, Liu JM, Yang B, 2021. Structure differences of water soluble polysaccharides in *Astragalus membranaceus* induced by origin and their bioactivity. *Foods*, 10(8):1755.
https://doi.org/10.3390/foods10081755

Song BC, Li P, Yan SJ, et al., 2022. Effects of dietary astragalus polysaccharide supplementation on the Th17/Treg balance and the gut microbiota of broiler chickens challenged with necrotic enteritis. *Front Immunol*, 13:781934.
https://doi.org/10.3389/fimmu.2022.781934

Song QB, Cheng SW, Li D, et al., 2022. Gut microbiota mediated hypoglycemic effect of *Astragalus membranaceus* polysaccharides in *db*/*db* mice. *Front Pharmacol*, 13: 1043527.
https://doi.org/10.3389/fphar.2022.1043527

Tamanai-Shacoori Z, Smida I, Bousarghin L, et al., 2017. *Roseburia* spp.: a marker of health? *Future Microbiol*, 12(2):157-170.
https://doi.org/10.2217/fmb-2016-0130

Thaiss CA, Zmora N, Levy M, et al., 2016. The microbiome and innate immunity. *Nature*, 535(7610):65-74.
https://doi.org/10.1038/nature18847

Turnbaugh PJ, Ley RE, Mahowald MA, et al., 2006. An obesity-associated gut microbiome with increased capacity for energy harvest. *Nature*, 444(7122):1027-1031.
https://doi.org/10.1038/nature05414

Ubeda C, Bucci V, Caballero S, et al., 2013. Intestinal microbiota containing *Barnesiella* species cures vancomycin-resistant *Enterococcus* faecium colonization. *Infect Immun*, 81(3):965-973.
https://doi.org/10.1128/iai.01197-12

Wang K, Liao MF, Zhou N, et al., 2019. *Parabacteroides distasonis* alleviates obesity and metabolic dysfunctions via production of succinate and secondary bile acids. *Cell Rep*, 26(1):222-235.e5.
https://doi.org/10.1016/j.celrep.2018.12.028

Wei XY, Tao JH, Xiao SW, et al., 2018. Xiexin Tang improves the symptom of type 2 diabetic rats by modulation of the gut microbiota. *Sci Rep*, 8:3685.
https://doi.org/10.1038/s41598-018-22094-2

Weiss GA, Chassard C, Hennet T, 2014. Selective proliferation of intestinal *Barnesiella* under fucosyllactose supplementation in mice. *Br J Nutr*, 111(9):1602-1610.
https://doi.org/10.1017/s0007114513004200

Wu MN, Li PZ, An YY, et al., 2019. Phloretin ameliorates dextran sulfate sodium-induced ulcerative colitis in mice by regulating the gut microbiota. *Pharmacol Res*, 150: 104489.
https://doi.org/10.1016/j.phrs.2019.104489

Wu TR, Lin CS, Chang CJ, et al., 2019. Gut commensal *Parabacteroides goldsteinii* plays a predominant role in the anti-obesity effects of polysaccharides isolated from *Hirsutella sinensis*. *Gut*, 68(2):248-262.
https://doi.org/10.1136/gutjnl-2017-315458

Wu X, Xu NN, Ye ZQ, et al., 2022. Polysaccharide from *Scutellaria barbata* D. Don attenuates inflammatory response and microbial dysbiosis in ulcerative colitis mice. *Int J Biol Macromol*, 206:1-9.
https://doi.org/10.1016/j.ijbiomac.2022.02.119

Yang XY, Jia CH, 2013. Understanding association of spleen system with earth on traditional Chinese medicine theory. *J Tradit Chin Med*, 33(1):134-136.
https://doi.org/10.1016/s0254-6272(13)60115-6

Yuan X, Chen RM, McCormick KL, et al., 2021. The role of the gut microbiota on the metabolic status of obese children. *Microb Cell Fact*, 20:53.
https://doi.org/10.1186/s12934-021-01548-9

Zaidi SJ, Husayni T, Collins MA, 2018. *Gemella bergeri* infective endocarditis: a case report and brief review of literature. *Cardiol Young*, 28(5):762-764.
https://doi.org/10.1017/s1047951118000070

Zhang L, Du JF, Yano N, et al., 2017. Sodium butyrate protects against high fat diet induced cardiac dysfunction and metabolic disorders in type II diabetic mice. *J Cell Biochem*, 118(8):2395-2408.
https://doi.org/10.1002/jcb.25902

Zhao WX, Cui N, Jiang HQ, et al., 2017. Effects of radix astragali and its split components on gene expression profiles related to water metabolism in rats with the dampness stagnancy due to spleen deficiency syndrome. *Evid Based Complement Alternat Med*, 2017:4946031.
https://doi.org/10.1155/2017/4946031

Zhao WX, Chen LJ, Cui N, et al., 2019. Polysaccharides from radix astragali exert immunostimulatory effects to attenuate the dampness stagnancy due to spleen deficiency syndrome. *Pharmacogn Mag*, 15(63):500-506.
https://doi.org/10.4103/pm.pm_503_18

Zhao WX, Wang T, Zhang YN, et al., 2022. Molecular mechanism of polysaccharides extracted from Chinese medicine targeting gut microbiota for promoting health. *Chin J Integr Med*, in press.
https://doi.org/10.1007/s11655-022-3522-y

Zhong MY, Yan Y, Yuan HS, et al., 2022. Astragalus mongholicus polysaccharides ameliorate hepatic lipid accumulation and inflammation as well as modulate gut microbiota in NAFLD rats. *Food Funct*, 13(13):7287-7301.
https://doi.org/10.1039/d2fo01009g

Zhou LJ, Liu ZJ, Wang ZX, et al., 2017. *Astragalus* polysaccharides exerts immunomodulatory effects via TLR4-mediated MyD88-dependent signaling pathway *in vitro* and *in vivo*. *Sci Rep*, 7:44822.
https://doi.org/10.1038/srep44822

Zhu LL, Sha LP, Li K, et al., 2020. Dietary flaxseed oil rich in omega-3 suppresses severity of type 2 diabetes mellitus via anti-inflammation and modulating gut microbiota in rats. *Lipids Health Dis*, 19:20.
https://doi.org/10.1186/s12944-019-1167-4

Supplementary information

Fig. S1; Table S1